Journal of Chromatography A, 1218 (2011) 5228–5234

Contents lists available at ScienceDirect

Journal of Chromatography A

journal homepage: www.elsevier.com/locate/chroma

Preparation and characterization of lauryl methacrylate-based monolithic microbore column for reversed-phase liquid chromatography

Shin Shu, Hiroharu Kobayashi, Norihisa Kojima, Akhmad Sabarudin, Tomonari Umemura*

Division of Nano-materials Science, EcoTopia Science Institute, Nagoya University, Furo-cho, Chikusa-ku, Nagoya 464-8603, Japan

ARTICLE INFO

Article history:
Received 22 March 2011
Received in revised form 27 May 2011
Accepted 31 May 2011
Available online 12 June 2011

Keywords:
Monolithic column
Microbore column
Lauryl methacrylate
Reversed-phase liquid chromatography
Inverse size exclusion chromatography

ABSTRACT

Poly(lauryl methacrylate-co-ethylene dimethacrylate) monoliths were in situ synthesized within the confines of a silicosteel tubing of 1.02 mm i.d. and 1/16″ o.d. for microbore reversed-phase HPLC. In order to obtain practically useful monoliths with adequate column efficiency, low flow resistance, and good mechanical strength, some parameters such as total monomer concentration (%*T*), cross-linking degree (%*C*) and polymerization temperature were optimized. High-efficiency monoliths were successfully obtained by thermal polymerization of a monomer mixture (40%*T*, 10%*C*) with a binary porogenic solvent consisting of 1-propanol and 1,4-butandiol (7:4, v/v) at a high temperature of 90 °C. The morphology and porous structure of the resulting monoliths were assessed by scanning electron microscope (SEM) and inverse size exclusion chromatography (ISEC), while the column performance was evaluated through the separations of a series of alkylbenzenes in acetonitrile–water (50:50, v/v) eluent. At a normal flow rate of 50 μL/min (corresponding to 1.66 mm/s), the optimized monolithic columns typically exhibited theoretical plate numbers of 6000 plates/10 cm-long column for amylbenzene ($k > 40$), and the pressure drop was always less than 1 MPa/10 cm. The monoliths, which were chemically anchored to the tube inner wall surface using a bifunctional silylation agent, exhibited adequate mechanical strength of up to 12–13 MPa, and were properly operated at 10 times higher flow rate than normal, reducing the separation time to one tenth. The lauryl methacrylate-based monolithic column was applied to a rapid and efficient separation of ten common proteins such as aprotinin, ribonuclease A, insulin, cytochrome c, trypsin, transferrin, conalbumin, myoglobin, β-amylase, and ovalbumin in the precipitation-redissolution mode. Using a linear CH_3CN gradient elution at a flow rate of 500 μL/min (10-times higher flow rate), 10 proteins were baseline separated within 2 min.

1. Introduction

Monolithic columns have gained greater acceptance as an alternative to traditional particle-packed columns due to the low flow-resistance and excellent mass transfer inherent in their configuration [1–3]. Hitherto, there have been numerous reports on polymer- and silica-based monolithic columns [4–9], and their applications have been extended from the original separation media to solid-phase extractors and microreactors [10–13].

While most of the work has focused on the development of capillary columns with internal diameters of approximately 75–250 μm [9,14–22], little work has been reported on the development of larger diameter monoliths of 0.5–1.5 mm i.d. [23–27]. This may be because capillary liquid chromatography (CLC) and capillary electrochromatography (CEC) using such a micro/capillary-scale column are well-suited to current needs in the growing life-science fields such as proteomics and metabolomics [28–31]. Another reason is that the liquid-molding process is essentially suitable for manufacturing narrow-bore columns [32]. In fact, it becomes increasing difficult to prepare larger-diameter homogeneous monoliths not only because of the unequal heating or UV radiation across the tube diameter but also because of the growing gravitational settling effect.

CLC and CEC have several important advantages over conventional HPLC including (1) minimum consumption of sample and reagents, (2) enhanced sensitivity from the limited sample volumes, (3) more efficient interfacing with mass spectrometry, and rapidly become an important analytical tool mainly in life science research. But, such capillary scale columns require dedicated HPLC equipments and some skills, which might slow down their widespread applications in other fields. In terms of practical usefulness for general HPLC users and also in the context of green chemistry, a little bit larger-diameter monolith, i.e., microbore columns with internal diameter of 1 mm may be preferable because the microbore column is applicable to commercially available standard HPLC system with minor modification [26].

* Corresponding author. Tel.: +81 52 789 5485; fax: +81 52 789 5485.
E-mail address: umemura@apchem.nagoya-u.ac.jp (T. Umemura).

0021-9673/$ – see front matter © 2011 Elsevier B.V. All rights reserved.
doi:10.1016/j.chroma.2011.05.104

The development of easy-to-use microbore columns may trigger the widespread use of monoliths among all the HPLC users. In the present work, thus, microbore monoliths (1 mm i.d.) were prepared by in situ polymerization of lauryl methacrylate with ethylene dimethacrylate in a silicosteel tubing (silica-coated stainless steel tube). Several parameters such as total monomer concentration (%*T*), cross-linking degree (%*C*), and polymerization temperature were optimized to obtain practically useful monoliths with low flow-resistance (less than 1 MPa at a normal flow rate), adequate separation efficiency (more than 5000 theoretical plates/column), and good mechanical strength (at least 10 MPa). The performance of the produced monolithic columns was evaluated through the separations of a series of alkylbenzenes and ten standard proteins.

2. Experimental

2.1. Apparatus

Microbore LC experiments were performed using a Shimadzu modular system equipped with a model LC-20AD pump, a model CBM-20A communication bus module, a Rheodyne 8125 injector with a home-made 1 μL loop, a model CTO-20AC column oven, and a model SPD-20A UV/VIS detector with a semimicro flow cell (2.5 μL). For the separation of proteins with a gradient elution, a gradient solvent delivery unit consisting of two Shimadzu LC-20AD pumps and a semi-micromixer (GL Sciences) with a volume of 10 μL was used. System control and data acquisition were conducted with Shimadzu LC solution software.

For inverse size exclusion chromatography (ISEC), another HPLC system also from Shimadzu was used. The system was composed of a LC-20AD pump, a SIL-20AC autosampler, a CTO-20AC column oven, and a SPD-20A UV/VIS detector. The mobile phase was tetrahydrofuran, and the injection volume of the autosampler was set at 1 μL. Detection was made at 254 nm, and the column temperature was maintained at 27 °C. The extra-column volume of the chromatographic system was measured to be 31 μL.

2.2. Chemicals

3-Methacryloxypropyltrimethoxysilane (MPS) was obtained from Shin-etsu Chemicals (Tokyo, Japan). Lauryl methacrylate (LMA) and ethylene dimethacrylate (EDMA) and 2,2′-azobisisobutyronitrile (AIBN) used as an initiator were purchased from Wako Pure Chemicals (Osaka, Japan). Organic solvents (1-propanol, 1,4-butanediol, ethanol, acetonitrile, acetone, and tetrahydrofuran) and trifluoroacetic acid (TFA) were also obtained from Wako Pure Chemicals. Uracil, alkylbenzenes and twelve polystyrene standards (MW = 500, 2000, 3000, 10 000, 20 000, 30 000, 70 000, 150 000, 300 000, 700 000, 1 000 000, 2 000 000) were purchased from Sigma–Aldrich Japan (Tokyo, Japan). Aprotinin (from bovine lung), ribonuclease A (bovine pancreas), insulin (bovine pancreas), cytochrome c (equine heart), trypsin (porcine pancreas), transferrin (human), conalbumin (chicken egg white), myoglobin (equine skeletal muscle), β-amylase (sweet potato), ovalbumin (chicken egg white) were obtained from Sigma–Aldrich (Steinheim, Germany). The water used throughout the present work was prepared using a Milli-Q purification system (Nihon Millipore Kogyo, Tokyo).

2.3. Preparation of lauryl methacrylate-based monolithic column

The monolithic columns were prepared by in situ polymerization within the confines of a silicosteel tubing. The procedure was almost the same as that described in previous reports [26,33]. In order to ensure covalent attachment of the monolith to the tube inner wall, the wall surface was treated with MPS before filling the polymerization mixture into the tube in the following way. Briefly, the silicosteel tubing was rinsed in sequence with Milli-Q water, 0.2 M NaOH, Milli-Q water, 0.2 M HCl, Milli-Q water and acetone using a syringe. The activated silicosteel tubing was then filled with a 30% MPS acetone solution, sealed with septa at both ends, and placed in an oven at 60 °C for overnight. After silanization, the silicosteel tubing with a vinylized inner surface was washed with acetone, dried using a stream of nitrogen, and sealed with septa until just before use.

The polymerization mixture was prepared in a glass vial by ultrasonically mixing LMA, EDMA, porogenic solvent, and AIBN in sequence, and the mixture solution was filled into the silanized silicosteel tubing, which was pre-cut to the desired length. After sealing of both ends, the tube was placed in an oven to proceeds the polymerization.

2.4. Characterization of monoliths

After all chromatographic experiments were completed, the monolith was removed from the column tubing by high pressure of over 20 MPa and dried in an oven at 90 °C for 24 h. The dried monolith was subsequently weighed and compared with the total weight of the feed monomer and cross-linker to obtain conversion percentage of monomer to polymer monolith. For all the monoliths examined, the conversion percentage exceeded 93% and the feed monomer and cross-linker were almost completely converted to polymer monolith.

Additionally, some parts of the monolith was cut to 1 cm length (25 mg) for nitrogen adsorption/desorption measurements with a BELSORP-mini II (Bel Japan Inc., Osaka, Japan), while the other part of the monolith was sputtered with gold for observation of morphology with a scanning electron microscope (SEM) (model S-3000 N, Hitachi High-Technologies Corporation, Tokyo, Japan).

3. Results and discussion

3.1. Preparation of poly(LMA/EDMA) monolith with higher hydrophobicity

High permeability of the monolithic columns allows rapid separation under very high flow-rate operation, while such monolithic columns are inevitably accompanied by a low phase ratio, leading to low retention factors [34]. In order to compensate the reduction of retention factors in reversed-phase mode, it is very important to prepare more hydrophobic monoliths. In the case of organic polymer monoliths, hydrophobicity (reversed-phase retention) may be improved by the use of more hydrophobic monomers, for example, methacrylate with a longer alkyl chain. However, the poor miscibility with porogenic solvent makes it difficult to prepare homogeneous monoliths [19,35]. Thus, in the present experiments, a widely accepted and convenient monomer, LMA, was chosen and in situ polymerized with EDMA, which is the most commonly used cross-linker.

The increase of %*T* is one of the most straightforward approaches to enhance the hydrophobicity and the resulting separation window, but higher %*T* leads to high flow resistance. The increase in the ratio of LMA to EDMA is also a promising approach, but the inevitable low-cross-linking may deteriorate the mechanical strength. Thus, the balance of %*T* and %*C* was first optimized in terms of high hydrophobicity (large separation window), adequate column efficiency, low flow-resistance, and good mechanical strength. The composition of the polymerization mixtures used in the present work is listed in Table 1. According to previous papers and our preliminary results [26,33], a mixture of 1-propanol and 1,4-butanediol was selected as a porogenic solvent. As mentioned

Table 1
Feed composition of the polymerization mixtures used in this experiment.

Monolith No.	Polymerization temperature (°C)	LMA (vol.%)	EDMA (vol.%)	1-Propanol (vol.%)	1,4-Butanediol (vol.%)
I	60	24.0	6.0	44.5	25.5
II	60	32.0	8.0	38.2	21.8
III	60	31.5	3.5	41.4	23.6
IV	90	31.5	3.5	41.4	23.6
V	70	36.0	4.0	38.2	21.8
VI	80	36.0	4.0	38.2	21.8
VII	90	36.0	4.0	38.2	21.8

The initiator, AIBN was added to the polymerization mixture at 1 wt.% of the total monomer content.

in some papers, column efficiency was improved with increasing the content of 1-propanol in the binary porogenic solvent, but the pressure drop became high, hampering rapid separation at a higher flow rate. Therefore, the volume ratio of 1-propanol to 1,4-butandiol was set at 7:4 so as to obtain adequate column efficiency as well as to minimize flow resistance.

Alkylbenzenes were used to evaluate the separation performance of the produced poly(LMA/EDMA) monoliths. The column length was 10 cm, and the column temperature was kept at 27 °C. For comparison with previous data, acetonitrile–water (50:50, v/v) was used as the eluent, and the flow rate was set at 50 μL/min (corresponding to 1.6–1.7 mm/s). Retention factors (k) for alkylbenzenes obtained under the above conditions were summarized in Table 2, together with the data on permeability (pressure drop at a constant flow rate) and column porosity. As expected, reversed-phase retention on the poly(LMA/EDMA) monoliths increased with increasing the %T and raising the ratio of LMA to EDMA. Also, it was clearly found that higher retention factors were obtained on the poly(LMA/EDMA) monoliths synthesized at higher polymerization temperature.

Here, reproducibility of the column preparation is a key factor for the use in routine analysis. Thus, three different monoliths of the same composition were prepared in the same manner, and the column-to-column reproducibility (monolith VII) was evaluated through the variation of retention time, retention factor, theoretical plate number, and pressure drop. The reproducibility was quite acceptable: the relative standard deviations (RSDs) of retention time and retention factor were found to be below 3%, while the RSDs values of theoretical plate number and pressure drop were within 10%.

The performance of the produced microbore columns was also compared with that of two commercially available silica-based C18 columns: L-column (10 cm long × 1.0 mm i.d., particle diameter of 3 μm, Chemicals Evaluation and Research Institute, Tokyo) and MonoBis (10 cm long × 1.0 mm i.d., monolithic column, Kyoto Monotech, Kyoto), as shown in Table 2. Generally, the amount of silica existing in a monolithic column is less than in a particle-packed column, leading to smaller surface area, which results in low retention factor. Then, the k values observed on the monolithic silica-C18 column (MonoBis) were smaller than those with particle-packed silica-C18 column (L-column) by a factor of 4. In contrast, the LMA-rich monolithic columns exhibited adequately high reversed-phase retention almost comparable to that with L-column.

It should be also noted here that the column porosities of the produced methacrylate monoliths was not so high (61.5–71.9%) compared with the value (81.6%) of the silica-based monolith (MonoBis), but their permeability was about 3 times higher. It may be a result of a high degree of connectivity among through-pores, which has been theoretically shown to be an important factor affecting the permeability of the monolith [36,37].

Some typical chromatograms obtained from the poly(LMA/EDMA)-based monolithic columns are shown in Fig. 1. The theoretical plate numbers for amylbenzene were estimated to be about 3000, 4000, 6000 and 6500 plates/10 cm for monolith I, III, IV, and VII, respectively. It is clearly seen that LMA-rich monoliths (monoliths IV and VII) polymerized at a high temperature of 90 °C exhibit better column efficiency reaching 6000 theoretical plates/10 cm at a pressure drop of less than 1 MPa.

3.2. Application of high flow rate for rapid separations

The low flow-resistance property of the poly(LMA/EDMA) monolith makes it possible to apply high flow rate, allowing high-speed separation. Thus, column efficiency at high flow rate and mechanical strength for high-pressure were examined in the flow rate range of 50–500 μL/min (corresponding to linear velocity of 1.66 mm/s to 16.6 mm/s). Fig. 2 shows typical chromatograms for the test mixture of five alkylbenzenes on (A) monolith I and (B) monolith VII at a flow rate of 500 μL/min. It can be seen that five alkylbenzenes are still baseline separated on both the columns.

Table 2
Characteristics of the produced monolithic columns.

Column	Retention factor, k					Theoretical plate numbers	Permeability[a]	Porosity[b] (%)
	Toluene	Ethylbenzene	Propylbenzene	Butylbenzene	Amylbenzene			
Monolith I[c]	2.59	3.82	6.09	9.8	15.5	2000–3000	0.4 MPa	71.9
Monolith II[c]	3.72	5.49	8.76	14.1	22.8	2000–3000	0.9 MPa	61.8
Monolith III[c]	4.15	6.43	10.8	18.2	30.0	3000–4200	0.5 MPa	66.3
Monolith IV[c]	4.39	6.88	11.6	19.6	32.5	5000–6500	0.6 MPa	67.0
Monolith V[c]	5.13	7.99	13.4	22.7	37.8	3000–4500	0.7 MPa	62.6
Monolith VI[c]	5.42	8.35	14.3	24.6	41.2	4500–6000	0.7 MPa	61.7
Monolith VII[c]	5.61	8.86	15.0	25.6	42.6	5000–7000	0.7 MPa	61.5
MonoBis[d]	2.04	3.24	5.52	9.37	15.9	6000–7200	2.3 MPa	81.6
L-column[e]	7.30	11.4	20.5	35.4	61.3	6500–7500	8.2 MPa	55.9

Mobile phase, acetonitrile–water (50:50, v/v); flow rate, 50 μL/min.
[a] Permeability (pressure drop) at a flow rate of 50 μL/min.
[b] The column porosity was calculated from the elution volume of the void marker, uracil.
[c] Column sizes for monoliths I–VII were 10 cm long × 1.02 mm i.d.
[d] MonoBis (column size, 10 cm long × 1.0 mm i.d., silica-based C18 monolithic column, Kyoto Monotech, Kyoto).
[e] L-column (column size, 10 cm long × 1.0 mm i.d., silica-based C18 packed column, 3 μm, Chemicals Evaluation and Research Institute, Tokyo).

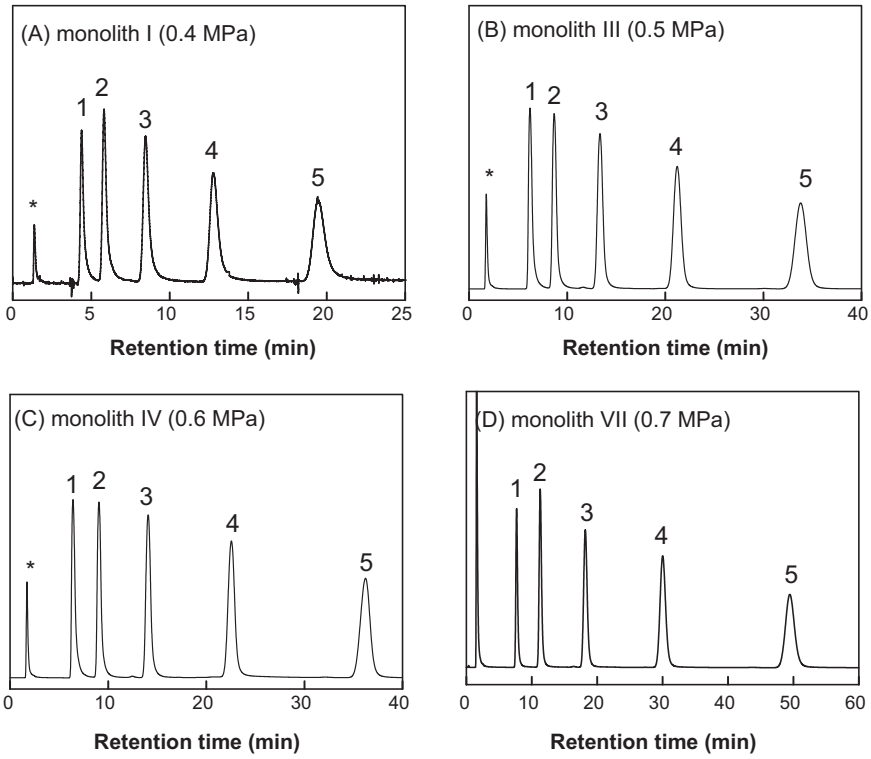

Fig. 1. Separations of a test mixture of five alkylbenzenes on 10 cm-long poly(LMA/EDMA)-based monolithic columns of (A) monolith I, (B) monolith III, (C) monolith IV, and (D) monolith VII. Column size: 10 cm long × 1.02 mm i.d.; mobile phase: acetonitrile–water (50:50, v/v); flow rates: 50 μL/min (corresponding to ca. 1.6 mm/s); injection volume: 1.0 μL; column temperature: 27 °C; UV detection at 214 nm. The pressure drop is denoted in the parenthesis. Peaks: (*) uracil, (1) toluene, (2) ethylbenzene, (3) propylbenzene, (4) butylbenzene, and (5) amylbenzene.

Fig. 3 shows van Deemter plots for amylbenzene, together with the data on pressure drop. Both the monolithic columns (I and VII) provided HETP values of tens of μm at a normal flow rate of 50 μL/min (1.66 mm/s), but there was a relatively steep loss of the efficiency along with increasing linear velocity, in contrast to the flat van Deemter profile observed with silica-based monoliths [38,39]. The deterioration in column efficiency at higher flow rate may be attributed to the inhomogeneity of the porous structure.

Then, the morphology and the through-pore size of the poly(LMA/EDMA) monoliths were further examined by scanning electron microscopy (SEM) and nitrogen adsorption–desorption measurements. SEM images of the monoliths are shown in Fig. 4. Typically, LMA-based monoliths polymerized at higher temperatures had more homogeneous skeleton. As can be seen in the comparison of Fig. 4(C) and 4(D), the optimized monolith (monolith VII) polymerized at a temperature of 90 °C is obviously more homogeneous, and the size of the globules was estimated to be 3 μm, which may produce the column efficiency similar to those of 3–5 μm particle-packed columns. Meanwhile, it was also found that the size of the flow-through path between the interconnected globules varied widely, ranging from a few to more than a dozen micrometers. These large through-pores and their high connectivity may produce low flow resistance, while the heterogeneity of the through-pores in size and shape cause a serious deterioration in column efficiency at higher flow rates.

As for the N_2 adsorption experiments, no obvious difference except specific surface area was observed: specific surface area, pore volume, and average pore size were 54.3 m^2/g, 0.09 cm^3/g, and 3.7 nm for monolith I, 57.1 m^2/g, 0.09 cm^3/g, and 3.7 nm for monolith V, and 60.2 m^2/g, 0.09 cm^3/g, and 3.7 nm for monolith VII, respectively.

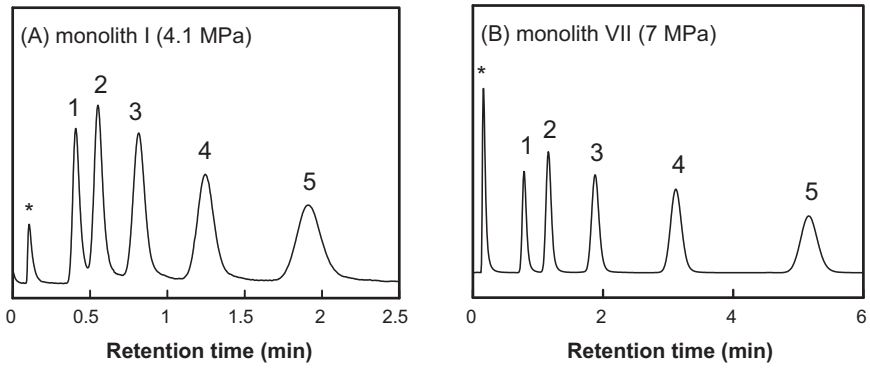

Fig. 2. Separations of a test mixture of five alkylbenzenes on 10 cm-long monolithic columns of (A) monolith I, (B) monolith VII at 10-times higher flow rate than normal. Flow rates: 500 μL/min (corresponding to ca. 16 mm/s). Other conditions are the same as in Fig. 1.

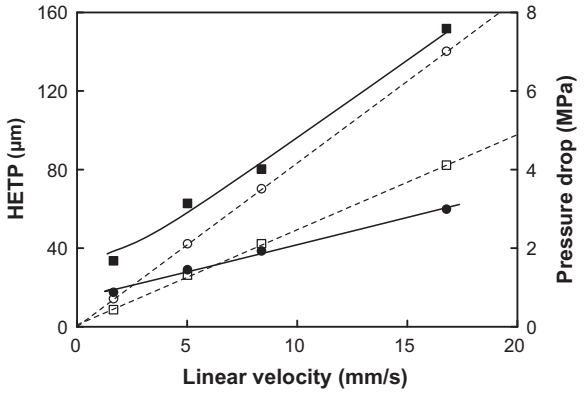

Fig. 3. Dependences of height equivalent to a theoretical plate (HETP) on the linear velocity of the mobile phase. □ monolith I, ○ monolith VII. Solid line for HETP, dashed line for pressure drop.

3.3. ISEC characterization of the poly(LMA/EDMA) monolith

To further characterize the porous structure of the produced poly(LMA/EDMA) monoliths, the porosity and pore size distribution were investigated by ISEC [40–43]. To differentiate the similar retention volumes of the polystyrene standards as much as possible, 30 cm long monolithic columns were specially prepared under the same polymerization conditions (monolith I and VII), and the ISEC plots for the poly(LMA/EDMA) monoliths were constructed according to the method described by Guan and Guiochon [40]. The ISEC plots are shown in Fig. 5. It should be first noted that there was a significant difference between the elution times of polystyrene standard with a molecular weight of 500 and toluene (total permeation volume marker), especially in the case of monolith VII. That kind of thing is common in organic polymer monoliths, and which is considered to be due to the existence of nanopores on the polymer surface [22,33]. In this regard, however, the longer retention of the toluene may not be due to permeation into the nanopores but due

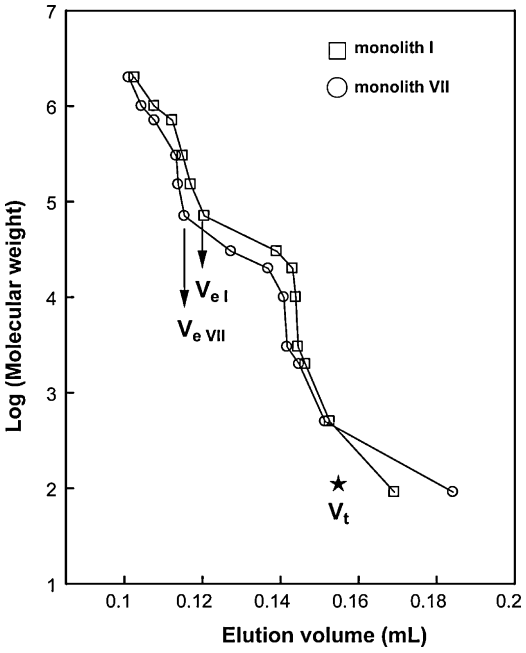

Fig. 5. Plot of the logarithm of molecular masses of polystyrene standards versus their elution volume. □ monolith I, ○ monolith VII. THF was used as the mobile phase at a flow rate of 50 μL/min. ⋆ Total permeation volume (V_t 0.154 mL) obtained from the elution volume of uracil in reversed-phase HPLC with acetonitrile–water (50:50, v/v).

to adsorption of sub-nm sized small toluene on the nanopores. In fact, total porosity (ε_t) calculated from the elution time of toluene in ISEC was 78.2% (for monolith VII), which was too high compared with the value anticipated from the percentage of the porogen content (60%) and the conversion percentage of the feed monomers to polymer monolith (93–97%). Thus, in the following calculations, the elution volume of uracil in a reversed-phase mode was used as

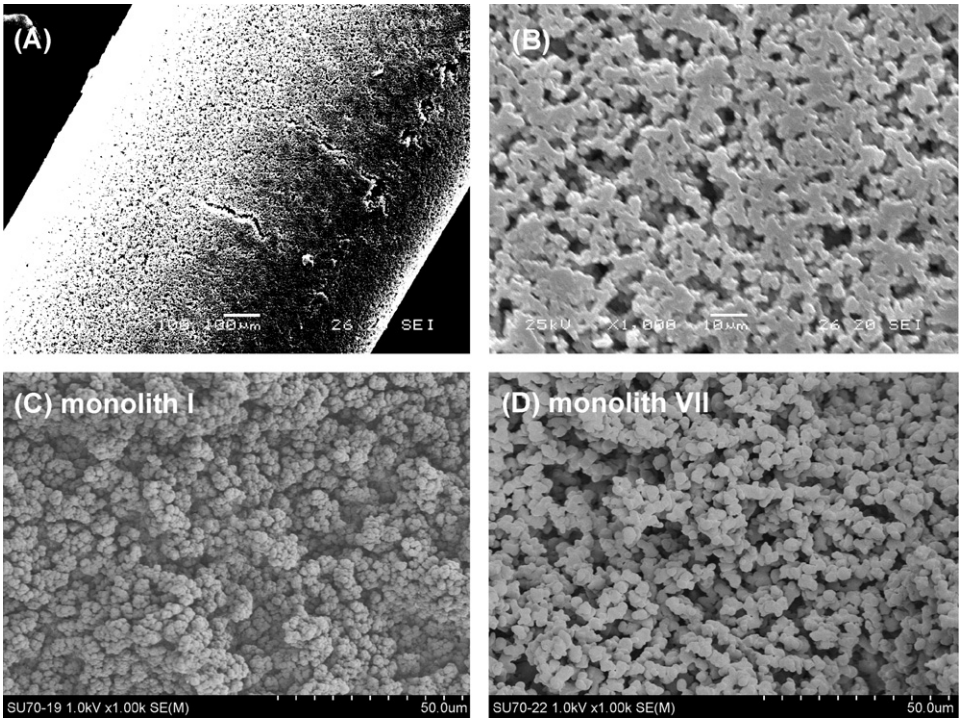

Fig. 4. Scanning electron microphotographs of monoliths. (A) 100× magnification of monolith VII slipped out of the column tubing, (B) 1000× magnification of monolith VII near the wall surface, (C) 1000× magnification of the cross section of monolith I, and (D) 1000× magnification of the cross section of monolith VII.

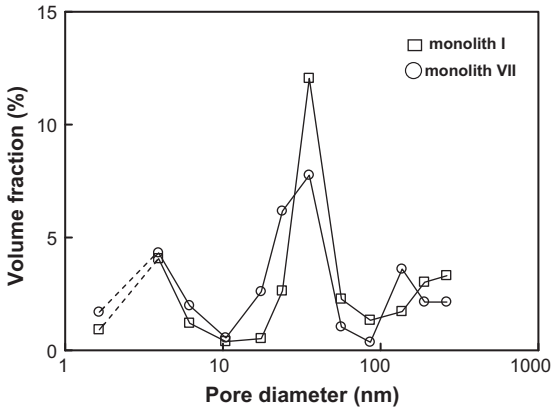

Fig. 6. Pore size distribution for monolith I and monolith VII.

an alternative to the total permeation volume. The elution volume was 0.154 mL and denoted by an asterisk in Fig. 5. Using this value (0.154 mL), the total porosity (ε_t) was re-calculated to be 65.4%, which may be plausible. The total (ε_t), external (ε_e) and internal (ε_i) porosities thus obtained were 65.4%, 49.0% and 16.4% for monolith VII and 65.4%, 51.4% and 14.0% for monolith I, respectively. "The increase in internal porosity was consistent with that in the specific surface area, leading to more efficient separation on the monolith VII"

The pore size distribution was also derived from the ISEC calibration curve, as shown in Fig. 6. There was a tendency that the optimized monolith (monolith VII) was rich in favorable mesopores especially in the range of 20–30 nm. In the case of monolith VII, the volume fraction for through-pores larger than 300 nm was found to accounted for 65.7%, while the fractions for pores (50–300 nm), mesopores (2–50 nm), and micropores (<2 nm) were estimated to be 8.24%, 24.4%, and 1.7%, respectively. It was confirmed that the optimized LMA-rich monoliths had large mesopore volume fractions comparable to those of silica-based monoliths.

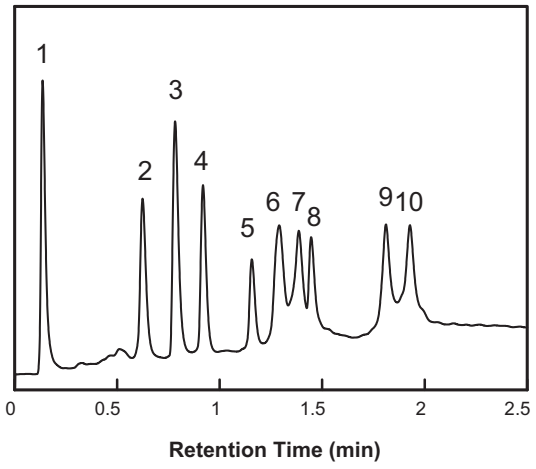

Fig. 7. Separation of 10 common proteins on 10 cm-long LMA-rich monolithic column by gradient elution with acetonitrile. Column: monolith VII (10 cm long × 1.02 mm i.d.); mobile phase: (A) 0.05% TFA aqueous solution, (B) 80% acetonitrile in 0.05% TFA aqueous solution; linear gradient: 20–100% (B) in 4 min; flow rate: 500 μL/min; column temperature: 20 °C; UV detection at 214 nm; injection volume: 1.0 μL; peaks: (1) aprotinin, (2) ribonuclease A, (3) insulin, (4) cytochrome c, (5) trypsin, (6) transferrin, (7) conalbumin, (8) myoglobin, (9) β-amylase, and (10) ovalbumin.

3.4. Separation of common proteins by a gradient elution

The produced LMA-rich monoliths exhibited adequate separation efficiency and mechanical strength, and then it is expected to be applied to rapid and efficient separation of proteins in precipitation-redissolution mode. Thus, its applicability was evaluated through the separation of ten common proteins. Fig. 7 shows the separation of ten proteins on a 10 cm-long LMA-rich monolith (monolith VII). The separation was performed using a simple linear gradient elution with acetonitrile in 0.05% TFA aqueous solution at a flow-rate of 500 μL/min (corresponding to a linear velocity of approximately 16.6 mm/s). As can be seen in Fig. 7, ten proteins were successfully separated within 2 min. It was confirmed that the produced LMA-rich monoliths allowed efficient separations of a large variety of compounds, ranging from small hydrocarbons to large biological molecules.

4. Conclusion

Practically useful microbore reversed-phase columns with adequate column efficiency (more than 5000 plates/10 cm) and low flow resistance (less than 1 MPa/10 cm) were reproducibly produced by in situ copolymerization of LMA and EDMA (40%*T*, 10%*C*) in the presence of 1-propanol and 1,4-butanediol (7:4, v/v) at a polymerization temperature as high as 90 °C. Batch-to-batch reproducibility of column fabrication was quite good with RSDs below 3%. The LMA-rich monoliths have great potential for separations of a variety of compounds from small analytes to large biomolecules, and may find various applications in biomedical and pharmaceutical analysis, process development, and environmental monitoring.

Acknowledgement

This work was supported by Industrial Technology Research Grant Program in 2007 (No. 07C46215a) from New Energy and Industrial Technology Development Organization (NEDO) of Japan and by Grant-in-Aid for Scientific Research (B) (No. 21350041) from Japan Society for the Promotion of Science.

Appendix A. Supplementary data

Supplementary data associated with this article can be found, in the online version, at doi:10.1016/j.chroma.2011.05.104.

References

[1] F. Svec, J.M.J. Fréchet, Science 273 (1996) 205.
[2] S. Hjerten, J.L. Liao, R. Zhang, J. Chromatogr. 473 (1989) 273.
[3] N. Tanaka, H. Kobayashi, K. Nakanishi, H. Minakuchi, N. Ishizuka, Anal. Chem. 73 (2006) 420A.
[4] N. Tanaka, H. Kobayashi, N. Ishizuka, H. Minakuchi, K. Nakanishi, K. Hosoya, T. Ikegami, J. Chromatogr. A 965 (2002) 35.
[5] H. Zou, X. Huang, M. Ye, Q. Luo, J. Chromatogr. A 954 (2002) 5.
[6] F. Svec, J. Sep. Sci. 27 (2004) 1419.
[7] K. Štulík, V. Pacáková, J. Suchánková, P. Coufal, J. Chromatogr. B 841 (2006) 79.
[8] E.G. Vlakh, T.B. Tennikova, J. Sep. Sci. 30 (2007) 2801.
[9] B.H. Gu, Z.Y. Chen, C.D. Thulin, M.L. Lee, Anal. Chem. 78 (2006) 3509.
[10] F. Svec, J. Chromatogr. A 1217 (2010) 902.
[11] Zhu, L. Zhang, H. Yuan, Z. Liang, W. Zhang, Y. Zhang, J. Sep. Sci. 30 (2007) 792.
[12] R. Wu, L. Hu, F. Wang, M. Ye, H. Zou, J. Chromatogr. A 1184 (2008) p369.
[13] T. Kubo, Y. Tominaga, K. Yasuda, S. Fujii, F. Watanabe, T. Mori, Y. Kakudo, K. Hosoya, Anal. Methods 2 (2010) 570.
[14] S. Eeltink, F. Svec, Electrophoresis 28 (2007) 137.
[15] J. Urban, P. Jandera, J. Sep. Sci. 31 (2008) 2521.
[16] X. Chen, H.D. Tolley, M.L. Lee, J. Sep. Sci. 32 (2009) 2565.
[17] Y. Ueki, T. Umemura, J. Li, T. Odake, K. Tsunoda, Anal. Chem. 76 (2004) 7007.
[18] L. Trojer, S.H. Lubbad, C.P. Bisjak, W. Wieder, G.K. Bonn, J. Chromatogr. A 1146 (2007) 216.
[19] Z.J. Jiang, N.W. Smith, P.D. Ferguson, M.R. Taylor, J. Biochem. Biophys. Methods 70 (2007) 39.
[20] Y. Huo, P.J. Schoenmakers, W.T. Kok, J. Chromatogr. A 1175 (2007) 81.
[21] T. Hirano, S. Kitagawa, H. Ohtani, Anal. Sci. 25 (2009) 1107.

[22] I. Nischang, O. Bruggemann, J. Chromatogr. A 1217 (2010) 5389.
[23] P. Coufal, M. Cihak, J. Suchankova, E. Tesarova, Z. Bosakova, K. Stulik, J. Chromatogr. A 946 (2002) 99.
[24] X.J. Huang, Q.Q. Wang, H. Yan, Y. Huang, B.L. Huang, J. Chromatogr. A 1062 (2005) 183.
[25] Z.D. Xu, L.M. Yang, Q.Q. Wang, J. Chromatogr. A 1216 (2009) 3098.
[26] T. Umemura, Y. Ueki, K. Tsunoda, A. Katakai, M. Tamada, H. Haraguchi, Anal. Bioanal. Chem. 386 (2006) 566.
[27] E.P. Nesterenko, P.N. Nesterenko, D. Connolly, F. Lacroix, B. Paull, J. Chromatogr. A 1217 (2011) 2138.
[28] S.H. Zhang, X. Huang, J. Zhang, C. Horváth, J. Chromatogr. A 887 (2000) 465.
[29] S.H. Zhang, J. Zhang, C. Horváth, J. Chromatogr. A 914 (2001) 189.
[30] A. Premstaller, H. Oberacher, W. Walcher, A.M. Timperio, L. Zolla, J.-P. Chervet, N. Cavusoglu, A. van Dorsselaer, C.G. Huber, Anal. Chem. 73 (2001) 2390.
[31] W. Walcher, H. Oberacher, S. Troiani, G. Hölzl, P. Oefner, L. Zolla, C.G. Huber, J. Chromatogr. B 782 (2002) 111.
[32] F. Svec, C.G. Huber, Anal. Chem. 78 (2006) 2100A.
[33] Y. Ueki, T. Umemura, Y. Iwashita, T. Odake, H. Haraguchi, K. Tsunoda, J. Chromatogr. A 1106 (2006) 106.
[34] T. Hara, H. Kobayashi, T. Ikegami, K. Nakanishi, N. Tanaka, Anal. Chem. 78 (2006) 7632.
[35] L. Trojer, C.P. Bisjak, W. Wieder, G.K. Bonn, J. Chromatogr. A 1216 (2009) 6303.
[36] J.J. Meyers, A.I. Liapis, J. Chromatogr. A 852 (1999) 3.
[37] A.I. Liapis, J.J. Meyers, O.K. Crossers, J. Chromatogr. A 865 (1999) 13.
[38] H. Minakuchi, K. Nakanishi, N. Soga, N. Ishizuka, N. Tanaka, Anal. Chem. 68 (1996) 3498.
[39] N. Tanaka, H. Nagayama, H. Kobayashi, T. Ikegami, K. Hosoya, N. Ishizuka, H. Minakuchi, K. Nakanishi, K. Cabrera, D. Lubda, J. High Resolut. Chromatogr. 23 (2000) 111.
[40] H. Guan, G. Guiochon, J. Chromatogr. A 731 (1996) 27.
[41] M. Al-Bokari, D. Cherrak, G. Guiochon, J. Chromatogr. A 975 (2002) 275.
[42] B.H. Gu, J.M. Armenta, M.L. Lee, J. Chromatogr. A 1079 (2005) 382.
[43] J. Urban, S. Eeltink, P. Jandera, P.J. Schoenmakers, J. Chromatogr. A 1182 (2008) 161.